Modeling and Simulation of Grid Connected Wind Energy Conversion System Based on a Doubly Fed Induction Generator (DFIG)

Chandrasekaran Subramanian, Domenico Casadei, Angelo Tani, and Claudio Rossi
Department of Electrical, Electronics and Information Engineering, University of Bologna, Bologna, Italy
Email: {chandras.subramanian, domenico.casadei, angelo.tani, claudio.rossi}@unibo.it

***Abstract*—This paper deals with the analysis, modeling, and control of a grid connected doubly-fed induction generator (DFIG) driven by the wind turbine. Recent advancements in size and technology of wind turbines require sophisticated control systems to effectively optimize energy conversion and enhance grid integration. This article investigates the power flow analysis of grid connected Wind Energy Conversion System (WECS) in a highly fluctuating wind environment. The WECS is equipped with a DFIG and a back-to-back converter in the rotor circuit. A control technique is presented for extracting the maximum power from the wind turbine. The grid side converter maintains the DC link voltage and the task of the rotor side converter is to track the maximum power point for the wind turbine. The description for the proposed system is presented with the detailed dynamic modeling equations. Simulation results for different operating conditions are presented.**

***Index Terms*—wind turbine, induction generator, power converter, modeling, control**

I. Introduction

Due to the economical and environmental benefits, Wind Energy Conversion System (WECS) have received tremendous growth in the past decade. The increased interest in wind energy has made it necessary to model and experimentally evaluate entire WECS, so as to attain a better understanding and to assess the performance of various systems. This paper describes a control strategy for a doubly fed induction generator (DFIG) with varying wind speed. Variable speed operation is essential for large wind turbines in order to optimize the energy capture under variable wind speed conditions. Variable speed wind turbines require a power electronic interface to permit connection with the grid. The power converter can be either partially rated or fully rated. A popular interface method for large wind turbines that is based on a partially rated converter is the doubly-fed induction generator (DFIG) system [1]. In the DFIG system, the power converter controls the rotor currents in order to control the electromagnetic torque and thus the rotational speed. Because the power converter only process the slip rotor power, which is typically 25% of the rated output power, the DFIG offers the advantages of speed control for a reduction in cost and power losses [2]-[3]. This paper presents a DFIG wind turbine system that is modeled in Matlab/Simulink and PLECS. A full electrical model is implemented that includes the power converter for the rotor side and a *dq* model of the induction machine. The aerodynamics of the wind turbine and the mechanical dynamics of the induction machine are included to extend the use of the model for variable wind speed conditions. For longer simulations that include these slower mechanical and wind dynamics, an averaged PWM converter model is presented. The averaged electrical model offers improved simulation speed at the expense of neglecting converter switching detail. The main feature of the implemented model is the possibility to investigate topics related to the diagnosis and Low Voltage Ride Trough (LVRT) capability of WECS. Simulation results for different operating conditions are presented in this paper, whereas the LVRT characteristics will be analyzed in a next paper.

Manuscript received February 6, 2013; revised August 7, 2014.

II. Modeling of the Wind Turbine System

Fig. 1 shows the overall schematic for DFIG based wind generation system. The system employs a back to back converter with reduced power rating. This bidirectional power converter consists of two conventional pulse-width modulated (PWM) inverters and is nowadays one of the most widely used converter topology in wind energy conversion system. The rotor side inverter is controlled so as to extract the maximum power from the wind turbine and to regulate the reactive power transferred to the utility grid. The main objective of the grid side inverter is the control of DC link voltage regardless of the wind speed. The DFIG is based on a wound rotor type induction machine. The torque speed profile of a typical induction machine with a short-circuited rotor is shown in Fig. 2. Thanks to the back-to-back converter that allows a bidirectional power flow between the rotor and the grid, the induction machine has two operating regions, i.e. sub synchronous and super

doi: 10.12720/ijoee.2.2.161-166

synchronous, that correspond to rotational speed below or above the synchronous speed.

The synchronous speed of the generator in rpm is defined by

$$n_s = \frac{f}{z_p} \times 60$$

where f is the grid frequency and Z_p is the number of pole pairs.

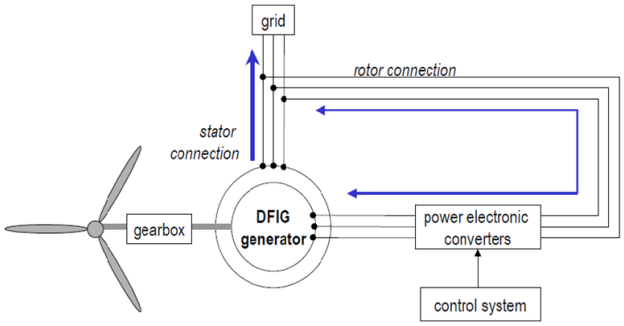

Figure 1. Schematic diagram of WECS

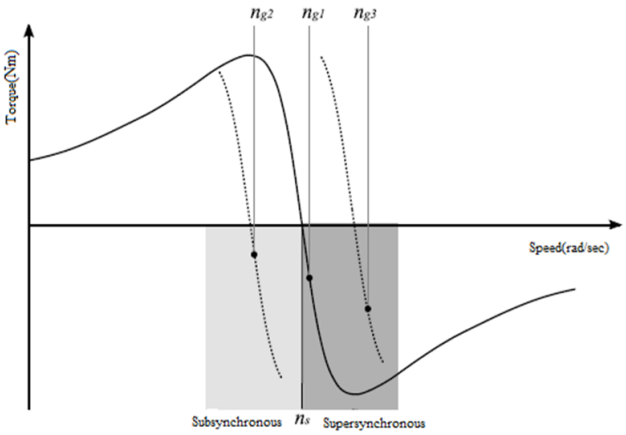

Figure 2. Torque-speed characteristics of induction machine

III. WECS Modeling

The simulation model takes into account the dynamics of the wind turbine, the mechanical and electrical dynamics of the induction machine, and the electrical dynamics of the grid and rotor side inverters and dc bus. Taking into account the slower dynamics of blade pitch control, it is assumed that the blade pitch angle remains constant and the wind speed never exceeds the rated value of 12m/s.

A. Wind Turbine Model

The wind turbine is modeled by converting the aerodynamic power created by the wind into a mechanical torque that drives the induction machine [3], [4]. The aerodynamic power, P_w, is calculated using (1).

$$P_w = 0.5\rho \times C_p(\lambda, \beta) \times V^3 A \quad (1)$$

and the mechanical torque is calculated with

$$T_m = \frac{P_w}{\omega_t} \quad (2)$$

$$T_m = 0.5\rho \times C_p V^3 \times \frac{60n}{2\pi n_g} \quad (3)$$

where ρ is the air density, n is the gearbox ratio, V is the wind velocity (m/s), A is the Swept area πr^2 (m^2) and n_g is the generator speed (rpm).

The performance characteristic, C_p, is approximated with the following equation:

$$C_P = 0.224\left(\frac{130}{\lambda} - 6.56\right)e^{-\frac{13.3}{\lambda}} \quad (4)$$

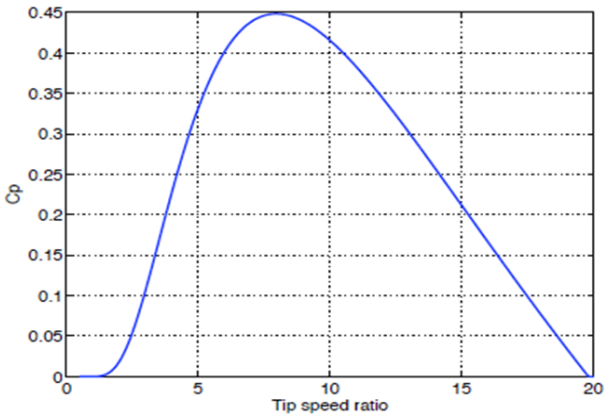

Figure 3. Wind turbine performance coefficient vs. tip speed ratio

The performance characteristic for the wind turbine is shown in Fig. 3. It can be seen that an optimal C_p of 0.45 exists at the optimal tip speed ($\lambda = r\omega/V$) ratio of 8.0. The torque model of the turbine, calculated from (3), is dependent on two variables, V and n_g.

B. DFIG Model

For a DFIG associated with a back-to-back converter on the rotor side and with the stator directly connected to the grid, an SFOC (stator flux oriented control) system is used in order to control separately the active and reactive power on the stator side. In the dq reference frame rotating synchronously with the stator flux, the stator voltages and fluxes can be written as follows [5]-[7]:

$$V_{ds} = R_s i_{ds} + \frac{d\varphi_{ds}}{dt} - \omega\varphi_{qs} \quad (5)$$

$$V_{qs} = R_s i_{qs} + \frac{d\varphi_{qs}}{dt} + \omega\varphi_{ds} \quad (6)$$

$$\varphi_{ds} = L_s i_{ds} + L_m i_{dr} \quad (7)$$

$$\varphi_{qs} = L_s i_{qs} + L_m i_{qr} = 0 \quad (8)$$

The last equation means that the d-axis is in phase with stator flux vector. In steady state conditions, by neglecting the stator phase resistance and by introducing the magnetizing current $i_{ms} = \varphi_s / Lm$, the stator voltage and current components become

$$V_{ds} \cong 0 \tag{9}$$

$$V_{qs} \cong |V_s| \cong \omega\varphi_{ds} \tag{10}$$

$$i_{ds} = \frac{L_m}{L_s}\left(i_{dms} - i_{dr}\right) \tag{11}$$

$$i_{qs} = -\frac{L_m}{L_s} i_{qr} \tag{12}$$

The active and reactive powers are as follows:

$$P_s = 1.5\left(V_{ds} i_{ds} + V_{qs} i_{qs}\right) \tag{13}$$

$$Q_s = 1.5\left(V_{qs} i_{ds} - V_{ds} i_{qs}\right) \tag{14}$$

By introducing (9)-(12) in (13) and (14), it is possible to rewrite the active and reactive power as function of stator voltage and rotor current components, leading to

$$P_s \cong -1.5|V_s| \times \frac{L_m}{L_s} i_{qr} \tag{15}$$

$$Q_s \cong 1.5|V_s| \times \frac{L_m}{L_s}\left(\frac{|V_s|}{2\pi f L_m} - i_{dr}\right) \tag{16}$$

By using (15) and (16) and assuming constant stator voltage magnitude V_s and frequency f, it is possible to consider the stator active power proportional to the q-axis rotor current component i_{qr} and the stator reactive power related to the d-axis rotor current component.

Electromagnetic Torque:

$$T_e = 1.5 z_p L_m \left(\varphi_{qs} i_{ds} - \varphi_{ds} i_{qs}\right) \tag{17}$$

where V_{ds}, V_{qs} are the stator voltage in the dq frame, i_{ds}, i_{qs} are the stator current in the dq axis, i_{dr}, i_{qr} are the rotor current in the dq frame, φ_{ds}, φ_{qs} are the stator flux in the dq frame, L_s is the stator inductance, L_m is the magnetising inductance and R_s is the stator resistance.

The mechanical dynamics of the rotor are represented using

$$\frac{d\omega_m}{dt} = \frac{1}{J}\left(T_e - F\omega_m - T_m\right) \tag{18}$$

where T_m is the external torque input from the wind turbine model, T_e is the electrical torque calculated in the electrical machine model, F is the coefficient of friction and J is the combined inertia of the rotor and turbine.

C. Power Converters Model

Two different converter models could be used in the simulation study; a switched 3 phase PWM converter model shown in Fig. 4 and an averaged PWM converter model shown in Fig. 5. The switched model is used to simulate the fast electrical dynamics of the system and the averaged model idealizes the switching action, making it suitable for longer simulations in which the slower mechanical and wind speed dynamics are studied [8-12].

With the averaged PWM converter model, the assumption is that the PWM is ideally imposed. The ac side voltages are therefore modelled as controlled voltage sources whose magnitude is calculated using

$$V_i = 0.5 m_i V_{dc} \tag{19}$$

where m_i is the modulation index of each converter phase. The dc side current is then calculated from the measured ac currents as follows:

$$I_{dc} = 0.5\left(m_a I_a + m_b I_b + m_c I_c\right) \tag{20}$$

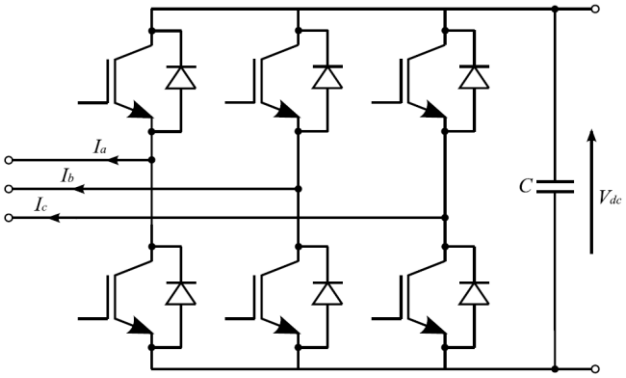

Figure 4. Switched PWM converter model

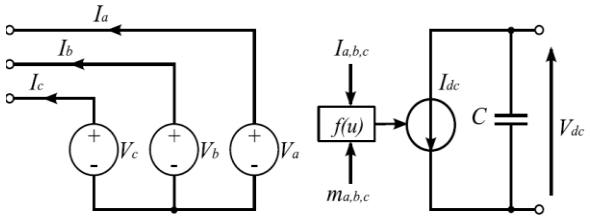

Figure 5. Averaged PWM converter model

IV. Control of WECS

The control block diagram of the DFIG system presented in the paper is shown in Fig. 6.

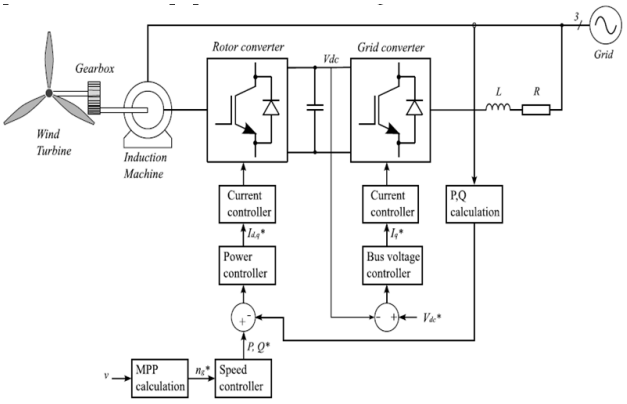

Figure 6. Control block diagram of DFIG

The rotor supply circuit comprises a grid side inverter and rotor side inverter that are linked via a dc bus. The dc bus capacitor decouples the two inverters, allowing them

to be independently controlled [12-15]. The parameters of the turbine and induction machine are given in Table I. The parameters have been adapted from a GE 1.5MW turbine [3]. It should be noted that the inertia was reduced by a factor of five in order to speed up the mechanical dynamic response of the turbine and allow for a faster simulation.

TABLE I. WECS PARAMETERS

Rated Power	1.5MW	Frequency	50Hz
Rated Voltage	575Vrms	Pole pairs	2
Stator resistance	1.4mΩ	Lm	1.53mH
Rotor resistance	0.99mΩ	Lr	1.61mH
Bus capacitance	38mF	Ls	1.62mH
Turbine radius	35m	Inertia	50kg.m^2

A. Grid Side Inverter (GSI) Control

The task of the grid side inverter is to regulate the voltage of the dc bus, V_{dc}. To achieve this, a voltage control loop controls the q-axis current, I_q* that affects the real power exported to or imported from the grid. The grid side converter can also be used for system power factor control by adding a reactive power control loop to control the d-axis current. In the example system, unity power factor operation is assumed and the d-axis current reference is therefore set to zero.

B. Rotor Side Inverter (RSI) Control

The purpose of the rotor inverter is to control the generator speed to achieve maximum power from the wind over a range of wind velocities. The rotor side inverter control scheme is based on a multitiered structure that comprises a speed, power and current control loop. It should be noted that omission of the power control loop is possible by implementing decoupled current control [8]. The reference speed for the outer speed control loop is determined by a maximum power point (MPP) calculation based on the wind velocity. Speed control is implemented by controlling the real power reference to the power control loop. In the power control loop, the reactive power reference is set to zero because it is assumed that the grid side converter will supply the needed reactive power to the system. The current controller tracks the power reference by controlling the rotor currents. Current control is performed in a *dq* reference frame that is rotating with the stator flux.

C. Operating Range

The output power of the wind turbine that is calculated using (1) and (4) is shown in Fig. 7 as a function of wind speed and generator rotational speed. It can be seen that the maximum output power of 1.5MW, generated at a wind speed of 12m/s, is harnessed at a generator rotational speed of 2000rpm. The wind turbine is not designed to produce a steady state output of more the 1.5MW. In practice, blade pitch control is used to reduce the aerodynamic power at higher wind speeds. Blade pitch control has been omitted from the turbine model since the focus of the simulation is on the faster electrical and motor dynamics.

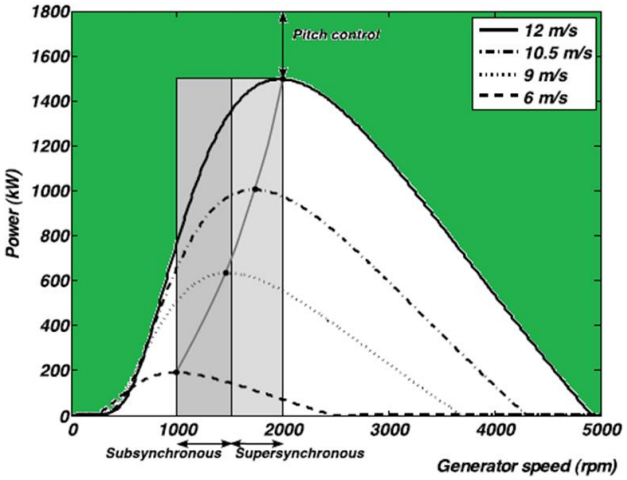

Figure 7. The maximum power point tracking (MPPT) for different wind speeds

D. Maximum Power Point Tracking (MPPT)

In the WECS system, maximum power tracking is Implemented using a simple technique that infers the optimal rotational speed of the generator, n_g*, from the wind speed measurement V [15-16]. The relationship between optimal generator rotational speed in rpm and wind speed is given in (21).

$$n_g^* = \frac{60\lambda_{opt} n}{2\pi R} \times V \tag{21}$$

where n is the gearbox ratio, V is the wind velocity (m/s), λ_{opt} is the optimal tip speed ratio and R is the radius of the blade (m).

V. SIMULATION RESULTS

Control loops are present in the DFIG system model that contains the averaged PWM converter model. The output states are directly dependent on the previous output due to the feedback based control loops. This forces Simulink to solve each simulation time step iteratively, slowing down the simulation. Memory blocks or low pass filters can be placed in the algebraic loop in order to rectify this problem. Since the simulation is configured for variable time step simulation, low pass filters are used to break the algebraic loop. Low pass filters produce more deterministic behaviour than a memory block in a variable step environment. Simulations of the proposed control strategy for a DFIG based wind energy generation system were carried out using Matlab/Simulink and PLECS. The DFIG is rated at 1.5MW, 575V (line), 50Hz, and its parameters are given in Table I.

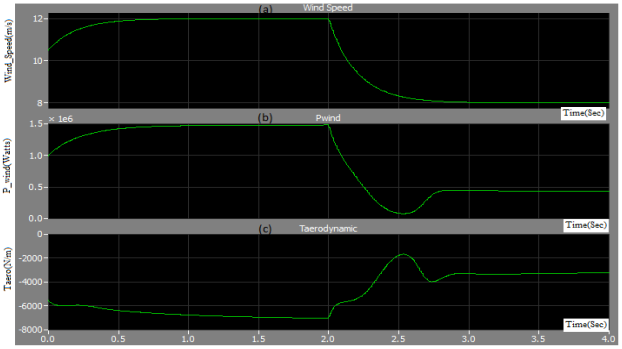

Figure 8.1. (a) Wind speed, (b) wind power, (c) aero. torque

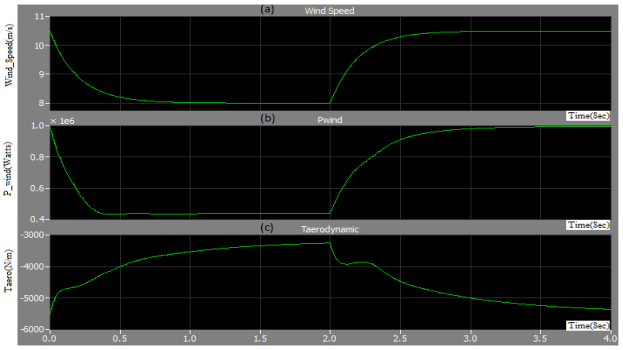

Figure 9.1. (a) Wind speed, (b) wind power, (c) aero. torque

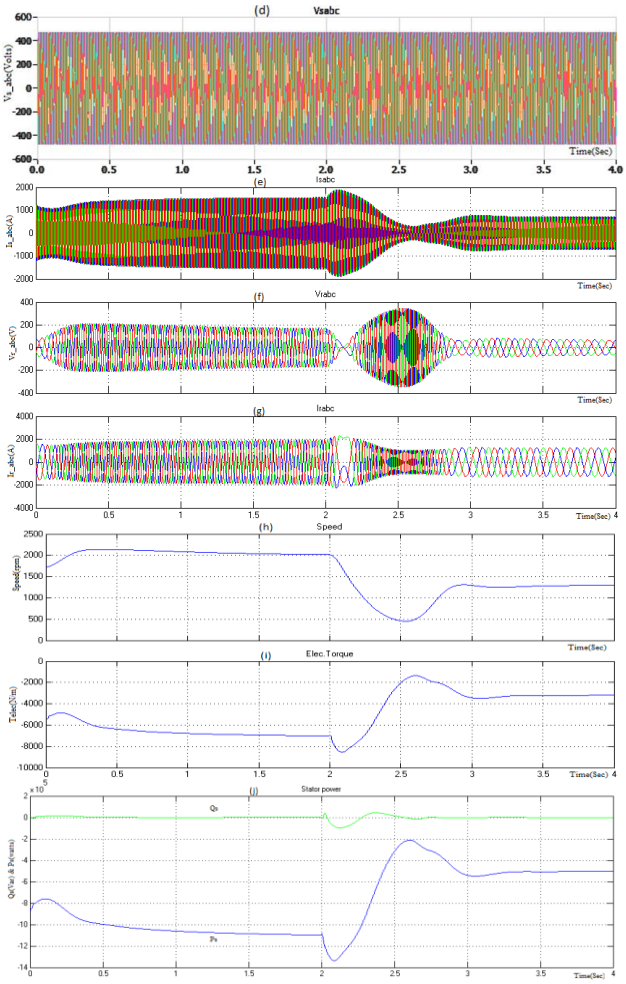

Figure 8.2. Simulation results of WECS for wind speed changing from 12m/s to 8m/s: (e) stator current, (f) rotor voltage, (g) rotor current, (h) generator speed, (i) electromagnetic torque, (j) stator reactive and active power

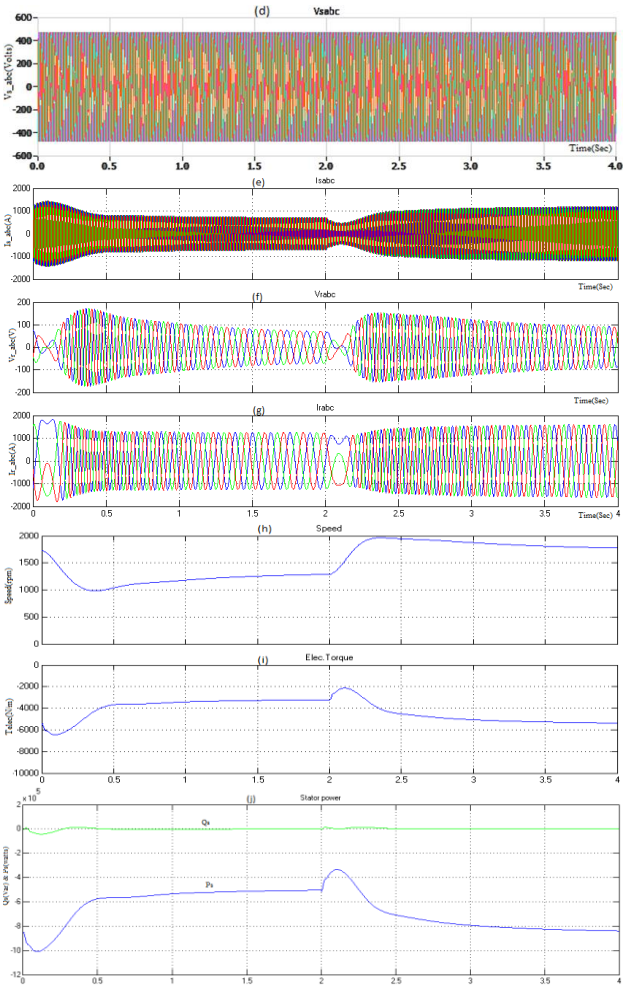

Figure 9.2. Simulation results of WECS for wind speed changing from 8m/s to 10.5m/s: (e) stator current, (f) rotor voltage, (g) rotor current, (h) generator speed, (i) electromagnetic torque, (j) stator reactive and active power

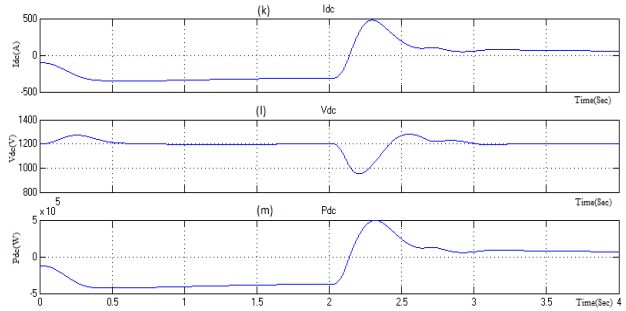

Figure 8.3. (k) DC bus current, (l) DC bus voltage, (m) P_{dc}

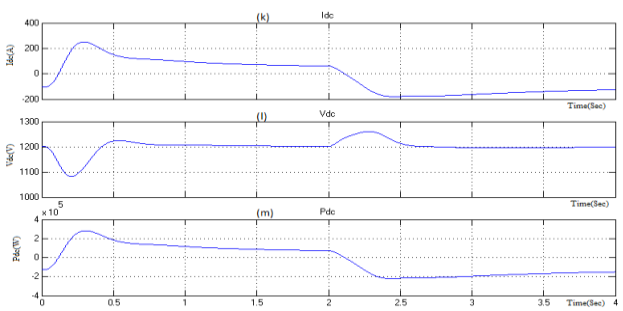

Figure 9.3. (k) DC bus current, (l) DC bus voltage, (m) P_{dc}

The waveforms in Fig. 8 and Fig. 9 show the simulation results of 1.5MW DFIG wind turbine with varying wind speed. The waveforms in Fig. 8.1 describe the wind speed, the power extracted from the wind and mechanical torque with the wind speed changing from 12m/s to 8m/s. From t=0.6s to t=2s, the machine operates at the wind speed of 12m/s. From t=2s to t=4s, the machine is subjected to operate with a wind speed changing from 12m/s to 8m/s. The corresponding stator current, rotor voltage and rotor current, electrical speed, torque, and stator power are presented from top to bottom in Fig. 8.2. The DC bus current, DC bus voltage and DC bus power are shown in Fig. 8.3.

The waveforms in Fig. 9.1 describe the wind speed, the power extracted from the wind and mechanical torque with the wind speed changing from 8m/s to 10.5m/s. From t=0.6s to t=2s, the machine operates at the wind speed of 8m/s. From t=2s to t=4s, the machine is subjected to operate with a wind speed varying from 8m/s to 10.5m/s. The corresponding stator current, rotor voltage and rotor current, electrical speed, torque, and stator power are presented from top to bottom in Fig. 9.2. The DC bus current, DC bus voltage and DC bus power are shown in Fig. 9.3. From the simulation results we have seen that there is a small transient occur at the change of wind speed this could be mitigated using averaged PWM converter.

REFERENCES

[1] S. Muller, M. Deicke, and R. D. Doncker, "Doubly fed induction generator systems for wind turbines," *IEEE Industry Applications Magazine*, vol. 8, pp. 26-33, Jun. 2002.

[2] R. Pena, J. C. Clare, and G. M. Asher, "Double fed induction generator using back-to-back PWM converter and its application to variable-speed wind-energy generation," *IEE Proceedings-Electric Power Applications*, vol. 143, no. 3, pp. 231-241, 1996.

[3] N. Miller, W. Price, and J. Sanchez Gasca, "Dynamic modeling of GE 1.5 and 3.6 wind turbine generators," *GE-Power Systems Energy Consulting*, 2003.

[4] Z. Lubosny, *Wind Turbine Operation in Electric Power Systems: Advanced Modeling*, Berlin: Springe Verlag, 2003.

[5] J. H. S. Hansen, M. Lau, and P. F. Sørensen, "Sensorless control of a double fed induction generator," Institute of Energy Technology, Aalborg University, 1999.

[6] C. Rossi, D. Casadei, F. Filippetti, A. Stefani, A. Yazidi, and G. A. Capolino, "Doubly-fed induction machines diagnosis based on signature analysis of rotor modulating signals," *IEEE Transactions on Industry Applications*, vol. 44, no. 6, pp. 1711-1721, Nov./Dec. 2008.

[7] Domenico Casadei, "Dinamica degli azionamenti elettrici," Dept. of Electrical, Electronics and Information Engineering, University of Bologna.

[8] E. Bogalecka, "Power control of a double fed induction generator without speed or position sensor," in *Proc. fifth European Conference on Power Electronics and Application*, Brighton, Sep. 1993, pp. 224-228.

[9] Bjørn Andresen, Eckardt Siebenthaler, and Lorenz Feddersen, "Variable speed wind turbine having a passive grid side rectifier with scalar power control and dependent pitch control," Canadian Patent Application CA2003/418561, Nov. 2003.

[10] N. Mohan, T. M. Undeland, and W. P. Robbins, *Power Electronics: Converters, Applications, and Design*, 3rd Ed., John Wiley & Sons Inc., Oct. 2002.

[11] Y. Tang and L. Xu, "A flexible active and reactive power control strategy for a variable speed constant frequency generating system," *IEEE Trans. on Power Electronics*, vol. 10, no. 4, pp. 472-478, Jul. 1995.

[12] S. K. Chung, "Phased-locked loop for grid-connected three-phase power conversion systems," *IEE Proceeding-Electric Power Applications*, vol. 147, no. 3, pp. 213-219, May 2000.

[13] J. I. Jang, Y. S. Kim, and D. C. Lee, "Active and reactive power control of DFIG for wind energy conversion under unbalanced grid voltage," in *Proc. IPEMC*, Shanghai, Aug. 2006, pp. 1-5.

[14] J. G. Slootweg, H. Polinder, and W. L. Kling, "Dynamic modeling of a wind turbine with doubly fed induction generator," in *Proc. Power Engineering Society Summer Meeting*, Vancouver, 2001, pp. 644-649.

[15] R. Datta and V. T. Ranganathan, "A method of tracking the peak power points for a variable speed wind energy conversion system," *IEEE Trans. on Energy Conversion*, vol. 18, no. 1, pp. 163-168, 2003.

[16] M. H. Hansen, A. D. Hansen, T. J. Larsen, S. Øye, P. Sørensen, and P. Fuglsang, "Control design for a pitch regulated, variable speed wind turbine," Risø report R-1500, Risø National Laboratory, Denmark, 2005.

